

# Non-Poisson Fluctuation Statistics In Neuronal Inter-Spike Intervals (ISI): Hurst parameter Estimates of Mouse Retinal Ganglion Signals

Q. Zhong\*, P. O. Boykin<sup>†</sup>, S. Nirenberg<sup>‡</sup>, V. P. Roychowdhury\*

\* Department of Electrical Engineering, University of California, Los Angeles, CA, USA

<sup>†</sup> Department of Electrical and Computer Engineering, University of Florida, Gainesville, FL, USA

<sup>‡</sup> Department of Neurobiology, University of California, Los Angeles, CA, USA

**Abstract**—There is considerable recent interest in both (i) modelling the retinal ganglion cells, so that the models can generate output that approximates the actual response of the retina (such models will help design retinal prosthetics); and (ii) understanding how relevant information is encoded in the spike patterns generated by the ganglion cells (these neuronal codes will help understand how the brain analyzes visual scenes). Since the signals (as captured by ISI) are fundamentally stochastic, any modelling or analysis tool will have to track, and make assumptions about, the fluctuations or noise inherently present in these signals. Even though there have been recent work claiming that the fluctuations are fractal in nature, showing long-range dependencies, almost all modelling and analysis work continue to assume Poisson fluctuations. The widespread use of the Poisson model is partly for the sake of convenience, and partly due to the fact that those claiming on fractal nature of ISI are contradictory: In [1] a long-range dependency (i.e., Hurst parameter [2],  $H > 0.5$ ) is claimed in cat's retina, and in [3] an  $H < 0.5$  and a long-range anti-correlation are claimed for paddlefish electroreceptors. We resolve this issue by studying the ISI of more than 50 ganglion cells recorded from two different mouse retinas, and (i) Conclusively show that the Hurst parameter is less than 0.5; we also show why the results presented in [1] are erroneous: methods that do not detrend the data were used. (ii) Even though the fluctuation function is scale free, the auto-correlation function of ISI does not show a long-range anti-correlation behavior as claimed in [3]. In fact, the auto-correlation function shows a sharp negative region around the origin, followed by an exponentially decaying tail. Our results generate questions about how the non-Poisson and scale-free nature of ISI fluctuations emerges during retinal processing, and how it might affect the accuracy of models based on Poisson assumptions.

## I. INTRODUCTION

The fractal analysis has been successfully applied to studying the traffic systems [4], [5], the economics [6], [7], and natural phenomena [2], [8] for a long time. And recently, it has been applied to various biological systems, such as the analysis of the DNA sequences [9], [10], the heartbeat series [11], [12], and the neural systems [1], [3], [13]. Researchers have obtained different Hurst parameters from different systems. In the case of the spike trains generated by retinal ganglion cells, as mentioned in the abstract, inconsistent results were reported [1], [3]. We feel there's a great need to clarify this fact, and we focus our research on the mouse visual neural system.

We investigated the Hurst parameter of the mouse visual neural system via both fluctuation analysis (FA) [8] and detrended fluctuation analysis (DFA) [9]. By comparing

the results from both methods, we found the true Hurst parameter; i.e., we conclude that there is significant trend in the ISI time series, and that the trend will cause FA to yield Hurst parameters that are significantly greater than 0.5, as reported in [1]. We first describe the data set in section II. Then in section III, we show the FA and DFA results of the neurons' ISI series. Specific simulations were carried out to clarify the contradiction coming from these two methods. And finally in section IV, we studied the autocorrelation function with different Hurst parameters, and show why the claim in [3] about long-range anti-correlation in ISI is fallacious.

## II. DATA DESCRIPTION

Mice were placed in the dark overnight before the experiment then killed with 100% CO<sub>2</sub>. The eye was then removed. And under dim red light (low-pass filter with a 580 nm cut off; intensity, 0.65 microwatts/cm<sup>2</sup> or 250 rod-equivalent photons/micron<sup>2</sup>/sec), the cornea, lens, and vitreous were removed and the retina was isolated from the pigment epithelium. A 2.5 × 2.5 mm piece was cut from the central retina and placed on a 64-electrode extracellular multielectrode array in a recording chamber where it was perfused continuously with oxygenated Ringer's solution throughout the experiment. The cells responses were then recorded simultaneously. The experiments were performed in accordance with UCLA animal research committee guidelines.

We analyzed two separate data sets, consisting of 17 and 36 retinal ganglion cells from two different mouse retinas respectively. All these cells were stimulated by the same stimulus, the full field of a computer monitor with a 256-value linear intensity scale (0 is darkest, 255 is brightest), driven by a series of Gaussian deviating with a mean of 127 and a standard deviation of 60 every 100 ms for 1.5 hour. We ordered the cells according to the ascending firing rate, which ranges from 4.2 Hz to 77.4 Hz in the first data set, and from 0.4 Hz to 43.9 Hz in the second data set.

## III. RESULTS

### A. FA and DFA analysis of the ISI series

The FA and DFA results of neuron 1 from the first data set are plotted in Fig. 1 respectively. It's observed that all DFA1-DFA7 give similar results, except that the "tail" in DFA1 has been gradually removed with higher order DFA,

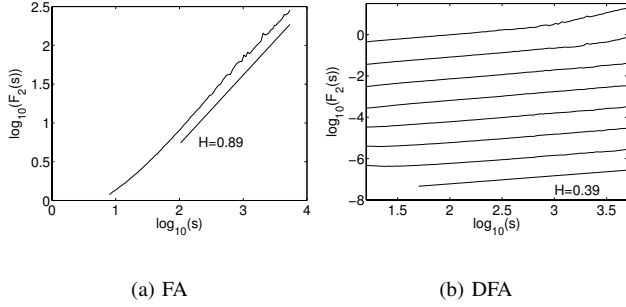


Fig. 1. a: FA result of neuron 1's ISI. b: DFA result of neuron 1's ISI. The fluctuation functions  $F_2(s)$  were obtained from the first, second, up to seventh order DFA (DFA1-7, from top to bottom, shifted vertically for clarity).

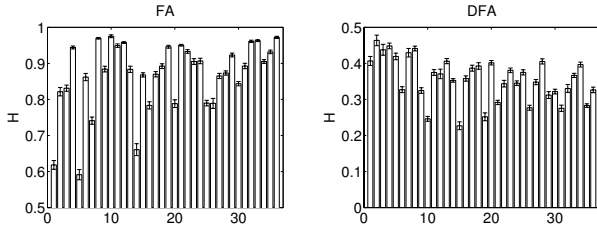


Fig. 2. FA and DFA results for the 36 ganglion cells in the second data set. Every bar represents a ganglion cell, which is ordered by the ascending firing rate. We gave the 95% confidence level for the exponents estimation.

which is a distinctive signature of the detrending process. Thus DFA7 was chosen to fit the exponent. Both FA and DFA lead to robust power law between  $s$  and  $F_2(s)$ ; however, with different slopes. While FA gives the Hurst parameter 0.89, DFA suggests  $H \approx 0.39$  instead.

The FA and DFA results for all neurons in the first data set are summarized in Table I. The 95% confidence level of the estimation is also given. As neuron 1, FA and DFA always give contradictory results: the results from FA range from 0.77 to 0.98; while those from DFA range from 0.31 to 0.44<sup>1</sup>. And similar to what's shown in Fig. 1, the power law is robust in both FA and DFA plots for all these neurons. We obtained similar pattern from the second data set, which consists of 36 cells stimulated by the same white Gaussian noise, displayed in Fig. 2. Then which method gives the true Hurst parameters? We turn into the next subsection for clarification.

### B. Are the real Hurst parameters larger or less than 0.5?

Our simulation began with the random shuffling test, which tells us whether a completely random process can assume the observed results or not. Then if an original series gives  $H$  as 0.8, and its shuffled series reports  $H$  as 0.5, the well separated two results indicate that the result of 0.8 Hurst parameter comes from the property of the original series.

<sup>1</sup>Note that DFA indicates that there're three cross-over neurons: 7, 9, and 13, whose Hurst parameter estimates before the cross-over points are given in Table I. However, DFA is not sensitive about the cross-over point, as reported in [14].

TABLE I  
HURST PARAMETER ESTIMATES OF THE FIRST DATA SET

Neuron	FA	DFA
1	0.90 ± 0.007	0.39 ± 0.004
2	0.94 ± 0.005	0.44 ± 0.012
3	0.98 ± 0.004	0.36 ± 0.007
4	0.96 ± 0.004	0.34 ± 0.006
5	0.77 ± 0.010	0.39 ± 0.009
6	0.88 ± 0.005	0.37 ± 0.011
7	0.85 ± 0.011	0.31 ± 0.021
8	0.89 ± 0.007	0.35 ± 0.007
9	0.94 ± 0.004	0.36 ± 0.012
10	0.95 ± 0.003	0.35 ± 0.007
11	0.91 ± 0.008	0.42 ± 0.006
12	0.84 ± 0.005	0.31 ± 0.009
13	0.90 ± 0.006	0.41 ± 0.011
14	0.85 ± 0.006	0.36 ± 0.003
15	0.91 ± 0.004	0.32 ± 0.006
16	0.95 ± 0.004	0.31 ± 0.003
17	0.86 ± 0.005	0.37 ± 0.006

However, after the random shuffling, both methods give the exponents close to 0.5. The detail figures are omitted due to lacking of space. Thus the shuffling process still could not tell us which method is correct.

Series with specific  $H$  were then generated for testing these two methods. If a series has Hurst parameter  $H$ , its frequency spectrum  $F(f)$  and its profile's frequency spectrum  $F_{profile}(f)$  [15]

$$\begin{aligned} F(f) &\propto f^{-0.5(2H-1)} \\ F_{profile}(f) &\propto f^{-0.5(2H+1)} \end{aligned} \quad (1)$$

respectively. Following [16], we generated a  $H = 0.3$  series of 16,384 frames, as shown in Fig. 3.

Nextly, an exponential trend  $exp(-10^{-4} * i)$  (an exponentially decaying transient) and a periodic trend  $sin(10^{-3} * i)$  were added to this series respectively. Obviously, the expected  $H$  of the new series should still be 0.3. It's observed that FA reports  $H \approx 0.90 - 0.95$ , while DFA7 gives  $H \approx 0.29 - 0.31$  in Fig. 3c and d per contra, which is similar to what has been seen in the real neuron data.

A 10,000-frame-segment of the profile from the artificial series ( $H = 0.3$ ) generated above is plotted in Fig. 4a. The way we generated the artificial series began with the Gaussian noise, then it wouldn't introduce any important trend. Thus the 7<sup>th</sup> order polynomial trend doesn't match the profile well. However, there is important polynomial trend in the profile of neuron 12 ( $H = 0.31$  via DFA) from the first data set, as given in Fig. 4b. Then the polynomial trend introduced during the experiment and the data recording process must have played an important role of leading to the contradiction in FA and DFA. In this case, DFA gives the true results by removing the trend at first, otherwise FA might always pick up the trend and reports spurious results. Ref. [1] analyzed the cat's visual system, which should be

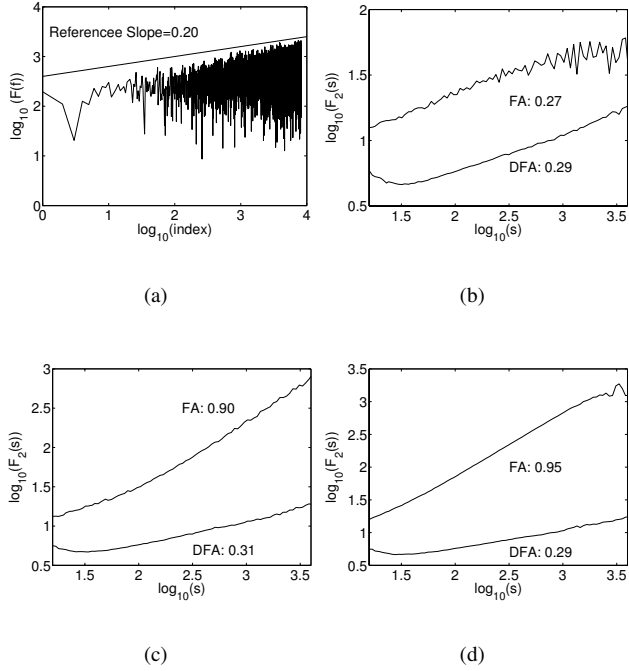


Fig. 3. a: The frequency spectrum of the artificial series with  $H = 0.3$ . b: FA and DFA results of this series. c: FA and DFA results of the series after an exponential trend is added. d: FA and DFA results of the series after being added a periodic trend.

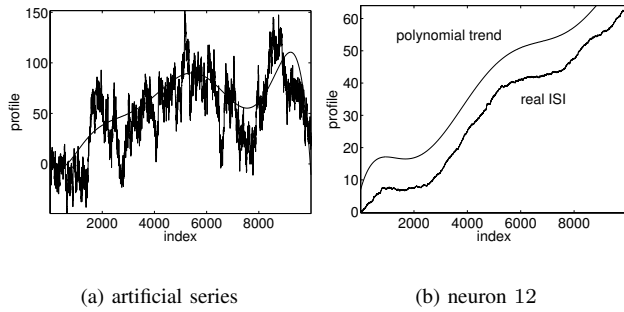


Fig. 4. A 10,000-frame-segment of the profile from the artificial series ( $H = 0.3$ ) and that from neuron 12 in the first data set. The trend of the real ISI was shifted vertically for clarity.

similar to the mouse visual system that we have analyzed, but reported the Hurst parameters to be larger than 0.5. Although [1] stimulated the retina with different stimulus (darkness, maintained light intensity, and a drift grating), the more likely reason for them to obtain the larger than 0.5  $H$  is because they didn't remove the trend in their analysis. Our results are consistent with [3], who obtained less than 0.5  $H$  when analyzing the paddlefish electroreceptors by DFA.

#### IV. DISCUSSION

People have understood the case when  $H \geq 0.5$  well, especially from the traffic engineering study. When  $0.5 < H < 1$ , it suggests the scale free autocorrelation pattern [15]

$$C(k) \sim k^{-(2-2H)}. \quad (2)$$

$C(k)$  here decays more slowly than  $k^{-1}$ , and the series is called a long-range correlated process. A  $H = 0.8$  series of 16,384 frames is plotted in Fig. 5a-b. When  $H = 0.5$ , it suggests no long-range relationship in the system, for an instance, the white Gaussian noise. Displayed in Fig. 5a-b, the randomly shuffled version of the series loses all its original correlation, leading  $H$  to be 0.5.

What remains unclear is the situation when  $H < 0.5$ . People believed that it suggested the long-range anti-persistence since otherwise  $H$  should end up with some value larger than or equal to 0.5. In addition, the profile looks noisy (small fluctuations go up and down as displayed in Fig. 4). Ref. [3] reported a long-range anti-correlation pattern, the sign changing alternatively and the magnitude decaying very slowly, found in paddlefish electroreceptors (see Fig. 1(c) in [3]) to account for the less than 0.5  $H$ . However, when we plotted the autocorrelation function of the series in Fig. 3a-b (both FA and DFA have proved its Hurst parameter to be around 0.3), we found that the autocorrelation begins with negative values in the first several lags, and can only be told from the shuffled series when  $k \leq 10$ .

We also analyzed series with similar autocorrelation pattern as shown in [3]. An autoregressive process of order 1 (AR(1) process)

$$x_i = \lambda x_{i-1} + \phi_i \quad (3)$$

might be a good start, where we chose  $\lambda = -0.8$ , and  $\phi_i$  to be a white gaussian noise process with variance 0.25. The

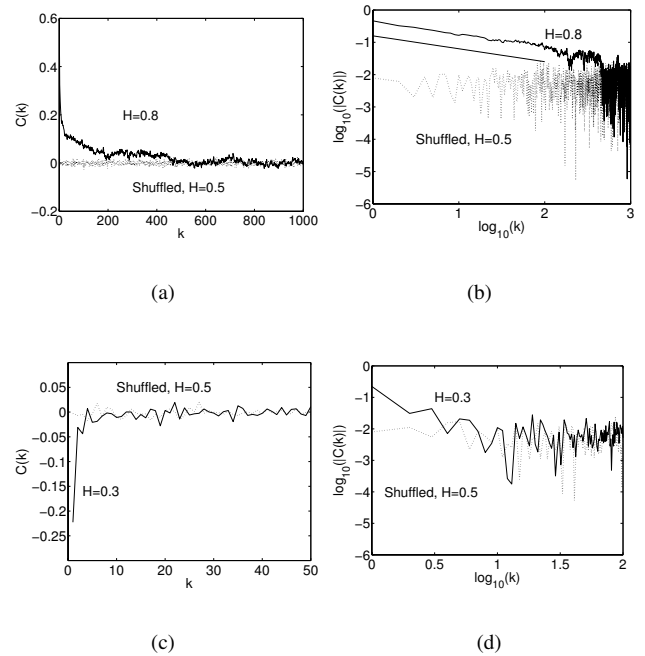


Fig. 5. a-b: The correlation for the series with  $H = 0.8$  is plotted in both natural and log-log scales. The reference line shown in (b) has slope  $-0.4 = -(2 * 0.8 - 1)$ . After being randomly shuffled, the series loses its long-range correlation. c-d: The correlation for the series with  $H = 0.3$ , as well as its randomly shuffled version, shown in both natural and double log scale.

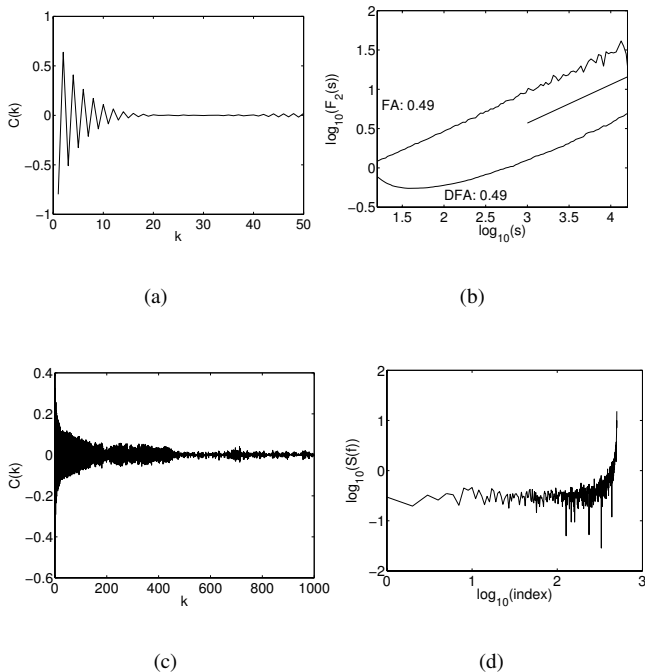


Fig. 6. a: The correlation function for an AR(1) process with  $\lambda = -0.8$ . b: The DFA and FA analysis results of this AR(1) process. c: The absolute value of the correlation is exactly what's shown in Fig. 7a, but starting from negative  $C(1)$ , we alternately change its sign to model a desired 'anti-correlation' series. d: The power spectrum of the series, shown in double log scale.

autocorrelation function of AR(1) process is known to be

$$C(k) \sim \lambda^k. \quad (4)$$

Thus with negative  $\lambda$ , the sign of the correlation changes alternatively, and the magnitude decreases as an exponential law, as shown in Fig. 6a. Both DFA and FA report  $H \approx 0.5$ , as expected for all AR(1) processes. We realized that [3] claimed a long-range, non-exponential anti-correlation in the neural ISI, thus we constructed the new correlation pattern in Fig. 6c, whose sign changes alternatively and magnitude decays as a power law, much more slowly than the exponential law observed in AR(1) process. We expected from (1) that the power spectrum of the series should be scale free, but we didn't observe this in Fig. 6d. This suggests that the autocorrelation pattern reported in [3] to be very spurious.

## V. SUMMARY

We have analyzed the mouse retina ganglion cells ISI with both FA and DFA. These two methods give inconsistent results: FA suggests Hurst parameters should be larger than 0.5, while DFA indicates they should be less than 0.5. Our further simulation has revealed the true Hurst parameters to be less than 0.5, and the reason FA reports wrong Hurst parameters is due to the trend existing in the real neuron data.

We have also revealed the autocorrelation pattern when  $H < 0.5$ : it is not a scale free anti-correlation pattern;

instead, the correlation function begins with negative values for several lags, and can only be differentiated from that of the shuffled series at the very beginning part.

Our future work might be to investigate the cause of the scale free property in the fluctuation function when  $H < 0.5$ . Furthermore, since FA and DFA only describe the second order fluctuation function of the neurons, we can also study the multifractality of the neurons through the Multifractal detrended fluctuation analysis (MF-DFA) [14].

## ACKNOWLEDGMENT

This work was supported in part by the NSF grant ITR 0326605. We would like to thank Adam Jacobs, who helped with the experiments involved in recording spike trains.

## REFERENCES

- [1] S. B. Lowen, T. Ozaki, E. Kaplan, B. E. A. Saleh, and M. C. Teich, "Fractal features of dark, maintained, and driven neural discharges in the cat visual system," *Methods*, vol. 24, pp. 377–394, 2001.
- [2] H. E. Hurst, "Long-term storage capacity of reservoirs," *Trans. Amer. Soc. Civ. Engrs.*, vol. 116, pp. 770–799, 1951.
- [3] S. Bahar, J. W. Kantelhardt, A. Neiman, H. H. A. Rego, D. F. Russell, L. Wilkens, A. Bunde, and F. Moss, "Long-range temporal anti-correlations in paddlefish electroreceptors," *Europhys. Lett.*, vol. 56(3), pp. 454–460, 2001.
- [4] W. E. Leland, M. S. Taqq, W. Willinger, and D. V. Wilson, "On the self-similar nature of Ethernet traffic," in *ACM SIGCOMM*, D. P. Sidhu, Ed., San Francisco, California, 1993, pp. 183–193. [Online]. Available: citeseer.ist.psu.edu/leland93selfsimilar.html
- [5] W. Willinger, M. S. Taqq, R. Sherman, and D. V. Wilson, "Self-similarity through high-variability: statistical analysis of Ethernet LAN traffic at the source level," *IEEE/ACM Trans. on Networking*, vol. 5, no. 1, pp. 71–86, 1997. [Online]. Available: citeseer.ist.psu.edu/willinger97selfsimilarity.html
- [6] B. B. Mandelbrot, "A multifractal walk down wall street," *Scientific American*, pp. 70–73, 1999.
- [7] E. E. Peters, *Fractal Market Analysis*. Wiley, 1994.
- [8] J. Feder, *Fractals*. New York: Plenum Press, 1988.
- [9] C. K. Peng, S. V. Buldyrev, S. Havlin, M. Simons, H. E. Stanley, and A. L. Goldberger, "Mosaic organization of DNA nucleotides," *Phys. Rev. E*, vol. 49(2), pp. 1685–1689, 1994.
- [10] A. Arnéodo, Y. d'Aubenton Carafa, B. Audit, E. Bacry, J. F. Muzy, and C. Thermes, "Nucleotide composition effects on the long-range correlations in human genes," *Eur. Phys. J. B*, vol. 1, pp. 259–263, 1998.
- [11] P. C. Ivanov, L. A. N. Amaral, A. L. Goldberger, S. Havlin, M. G. Rosenblum, Z. R. Struzik, and H. E. Stanley, "Multifractality in human heartbeat dynamics," *Nature*, vol. 399(6735), pp. 461–465, 1999.
- [12] A. L. Goldberger, L. A. N. Amaral, J. M. Hausdorff, P. C. Ivanov, C. K. Peng, and H. E. Stanley, "Fractal dynamics in physiology: Alterations with disease and aging," *Proc. Natl. Acad. Sci. USA*, vol. 99, pp. 2466–2472, 2002.
- [13] S. Blesić, S. Milošević, D. Stratimirović, and M. Ljubisavljević, "Detrended fluctuation analysis of time series of a firing fusimotor neuron," *Physica A*, vol. 268, pp. 275–282, 1999.
- [14] J. W. Kantelhardt, S. A. Zschiegner, E. Koscielny-Bunde, S. Havlin, A. Bunde, and H. E. Stanley, "Multifractal detrended fluctuation analysis of nonstationary time series," *Physica A*, vol. 316, pp. 87–114, 2002.
- [15] S. Havlin, R. B. Selinger, M. Schwarz, H. E. Stanley, and A. Bunde, "Random multiplicative processes and transport in structures with correlated spatial disorder," *Phys. Rev. Lett.*, vol. 61(13), pp. 1438–1441, 1988.
- [16] G. Rangarajan and M. Ding, "Integrated approach to the assessment of long range correlation in time series data," *Phys. Rev. E*, vol. 61(5), pp. 4991–5001, 2000.